Geological storage of CO_2: heterogeneity impact on pressure behavior

February 25, 2012

Contents

Abstract

Due to the high rates of industrial CO_2 emission, it is an operational obejectiv to maximize CO_2 injection rate into underground geological formations. Forcing the injection wells with high volumetric rates can result in an overpressurized system with possible breakings in the formation integrity, which increases the risk of CO_2 leakage.

The goal of this study is to investigate the injection pressure considerations that are needed to avoid uncontroled development of fractures in the medium. Herein, we study how the geological heterogeneity influences the pressure behavior of a typical CO_2 injection operation. Five variable geological features are considered as input for sensitivity analysis. These features span a realistic geological space.

Two injection scenarios are examined. In the first scenario, CO_2 is injected at a constant rate and the pressure in the well and the domain is allowed to build up unlimitedly. In the second scenario, a pressure constraint is set on the well, and the injection rate is changed to keep the pressure below the limit. Model responses related to pressure build-up and propagation within the system are defined and demonstrated for a selected case. Results for all cases are presented and discussed accordingly. We conclude by ranking the most influential geological parameters.

1 Introduction

The increasing level of green-house gases in the atmosphere, and in particular carbon dioxide, is believed to cause global climate changes. The industrial emission rate is expected to increase over the next decade, without taking necessary preventive actions. For example, according to the Energy Information Administration (EIA), the US carbon dioxide emissions are forecast to reach 6.41 billion tonnes by 2030. The Kyoto protocol proposed an emission cut which requires 1.75 billion tonnes of annual carbon dioxide reduction [10].

Geological storage of CO_2 is a proposed solution to fight global climate change. Clear operational criteria and policies must be made for the process to avert unwanted consequences. Concerns connected to putting a large mass of CO_2 into underground geological formations are not limited to the spatial distribution of the injected fluid. The pressure signals imposed through the injection point can travel beyond the scale of the CO_2 invaded zones. Although geological barriers can hinder the pressure exchange between different regions, pressure can transfer through low-permeable rocks where the CO_2 is trapped by capillarity.

In addition to the depleted oil and gas fields, deep geological aquifers are practical targets for geological storage of CO_2. If injecting into brine aquifers, the pressure waves can push brine into connected fresh water aquifers and contaminate them. Brine displacement issues are discussed in [4] by defining open, closed, and semi-closed aquifer boundaries. Brine might also leak through abandoned wells into other zones. Cailly et al. [3] discuss well design considerations to prevent any leakage through wells.

Geomechanical deformations are important during injection period. They can lead to changes in effective permeability and porosity. It is possible that the pressure build-up around injection wells will crack the rock with uncontrolled fracture extensions to the structural sealing layers. Faults can be activated due to high pressure in the system, providing a leakage path across layers. In addition to increased spatial CO_2 spread, an intensive induced fracture network can result in local earthquakes.

Pressure constraints must be considered for injection operations to limit the pressure buildup. However, this comes with the cost of injection rate reduction. Rock quality within the injection region has significant impact on pressure build up and therefore, geological uncertainty plays a considerable role in assessing the success and feasibility of the operation.

Any risk of breakings in the formation integrity must be assessed to define the appropriate preventive measures. We need to perform pressure sensitivity analysis to identify the influential parameters in the model. Uncertainty reduction in the influential parameters enhances the accuracy of pressure behavior prediction.

Geological uncertainty is a major issue in pressure analysis. Most of the pressure-related studies in the literature provide either deterministic case studies or generic preventive measures based on theoretical studies [9, 13, 6, 14, 12, 11]. It is important to include realistic geological descriptions in any study related to uncertainty. For example, permeability variation on the grid should be in the form of realizations of geological realistic formations. To the best of our knowledge, this is the first pressure study in the context of CO_2 storage that considers the geological uncertainty in the form of stractural variables rather than engineering parameters, such as permeability and porosity.

Within oil recovery context, the impact of geological uncertainty is thoroughly investigated in the SAIGUP project for shallow-marine depositional systems [5, 7, 8]. In the SAIGUP study, variations of geological features are examined in a set of field development strategies via several injection/production patterns. The study concludes that geological uncertainty has a dramatic influence on the oil recovery estimates. A number of geological realizations from the SAIGUP are used in [1, 2] to investigate the impact of geological uncertainty on injection and early migration of CO_2. Certain structural features are considered for those studies and flow responses are defined to measure the storage capacity, the trapping efficiency, and the leakage risk and the sensitivity of these responses to variations in geological parameters is investigated. Large variation in responses are observed. Aggradation angle and barriers are recognized to be the most influential in the CO_2 flow behavior[1, 2]. The focus in [1, 2] is to measure the spatial CO_2 distribution sensitivity to the variation of geological description.

This study is complementing [1, 2], in the sense that we herein analyze the sensitivity of pressure to the same geological parameters. In addition to the injection scenario used in [1, 2], we examine a different injection scenario with more realistic well control for the injection operation. A detailed study is given for the pressure behavior during injection time.

2 Geological parameters

In the SAIGUP study, a large number of realistic realizations were generated based upon a parametrization of a set of carefully selected geological features and a detailed sensitivity analysis study is performed for field oil recovery over number of development scenarios. Both the sedimentological and structural geological parameters have shown to dominate the uncertainty in total oil production. Hence, more accurate geological description enhances the quality of flow simulations.

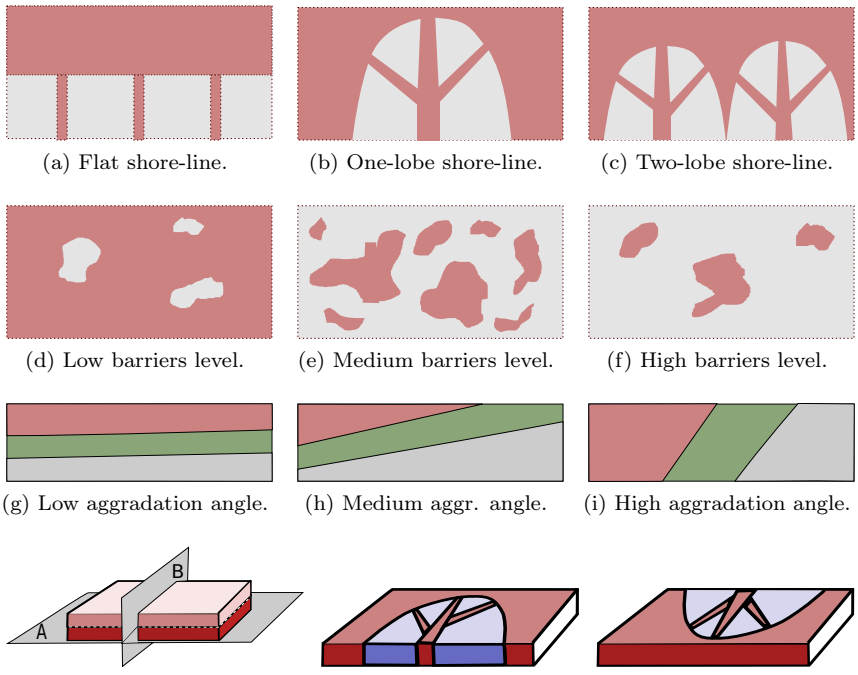

(a) Flat shore-line. (b) One-lobe shore-line. (c) Two-lobe shore-line.

(d) Low barriers level. (e) Medium barriers level. (f) High barriers level.

(g) Low aggradation angle. (h) Medium aggr. angle. (i) High aggradation angle.

(j) Slice A is used in Figures a-f and B in Figures g-i. (k) Updip progradation. (l) Downdip progradation.

Figure 1: The studied geological features. a-c) Shoreline shape, gray is for poor quality rock and brown color resembles a good quality rock. d-f) Barriers level defined by transmissibility multiplier. Gray color is for zero and brown color shows one. g-i) Aggradation angle. k-l) Progradation direction.

We have selected five geological parameters from the SAIGUP project to study the impact of heterogeneity

Table 1: Marker codes used in the result plots. The code level corresponds to levels in Figure 1.

Code	Description	Code level	Feature level
Thickness	Fault	thin/medium/thick	unfaulted/open/close
Shape	Lobosity	square/circle/diamond	flat/one-lobe/two-lobe
Size	Barriers	small/medium/large	10% / 50% / 90%
Color	Aggradation	blue/green/red	low/medium/high
Case no. counting	Progradation	first half/second half	up-dip / down-dip

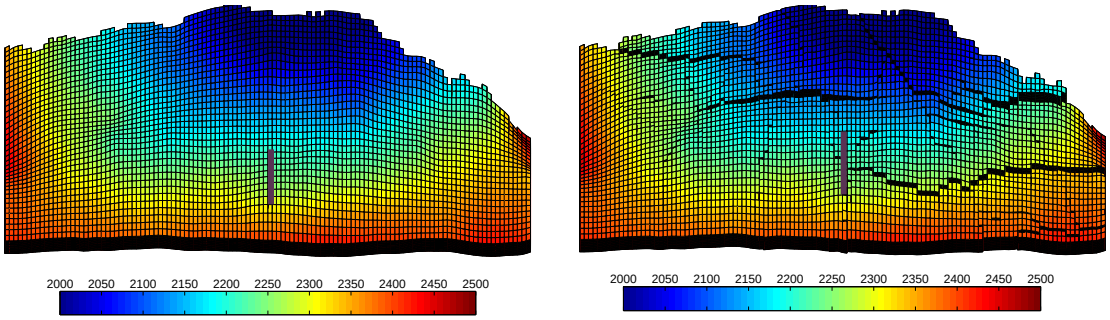

(a) Unfaulted grid.

(b) Faulted grid.

Figure 2: Models used in the study. Depth in meter is shown by color.

on the pressure responses in a typical CO_2 injection problem. These parameters span realistic intervals for progradational shallow-marine depositional systems with limited tidal influence. The considered features with the grading levels in each one, are shown in Figure 1. In addition to the features shown in Figure 1, we also consider faulting levels: unfaulted, open faults, and close faults. In subsequent plots, each of these features are represented with codes such as shape, size and color which are explained in Table 1. For more details refer to [1].

3 Injection scenario

We define a CO_2 injection scenario to be implemented for all cases in which we use an injector down in the flank and hydrostatic boundary conditions on the sides, except the side near the crest (see Figure 2). No-flow boundary conditions are imposed on the top and bottom surfaces of the model. Model dimensions are: 9km $\times$ 3km $\times$ 80m. The well is completed only in the four layers in all cases. The idea is to inject as low as possible to increase the travel path and the volume swept by the plume. If the medium is homogeneous, following the injection we expect one big plume to be constructed and this plume to move up due to the gravity force until it accumulates under the structural trap beneath the cap-rock.

Slightly compressible supercritical CO_2 is considered and we seek to inject a volume of 40MM m^3, which amounts to 20% of the total pore volume of the models. After the injection period, early plume migration is simulated in all of the studied cases and the simulation ends at 100 years. We use Corey-type quadratic functions for relative permeability, with end points 0.2 and 0.8 in both phases.

Low well injectivity can result in high pressure in the system. In this study, two injection strategies are implemented. In the first strategy (which is similar to the one used in [1]), the entire CO_2 volume is injected within 30 years at a constant volumetric rate. In the second strategy, we set an operational pressure constraint on the injector and continue injecting with appropriate rates to keep the pressure within the limit. We do some pressure response calculations to see the propagation of pressure pulses in the medium for both strategies.

In the pressure-constrained strategy, the injector operates with the priority of injecting a volumetric rate of 3650 m^3/day. A pressure constraint of 400 bar is set on the injector. If the well bottom-hole pressure goes higher than that and violates this restriction (to maintain the target injection rate), the priority changes

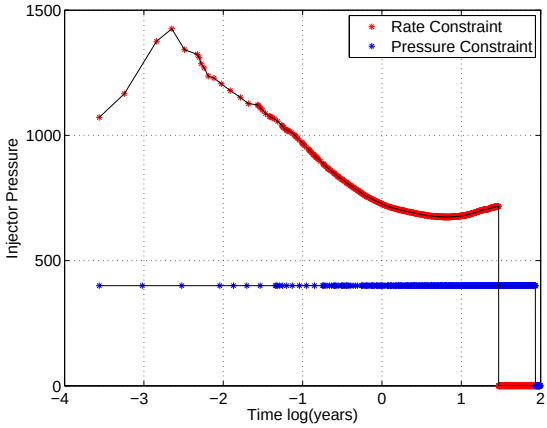

(a) Pressure in the injector versus logarithm of time.

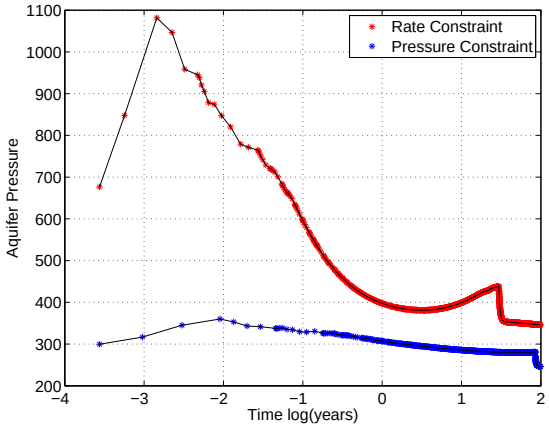

(b) Average aquifer pressure versus logarithm of time.

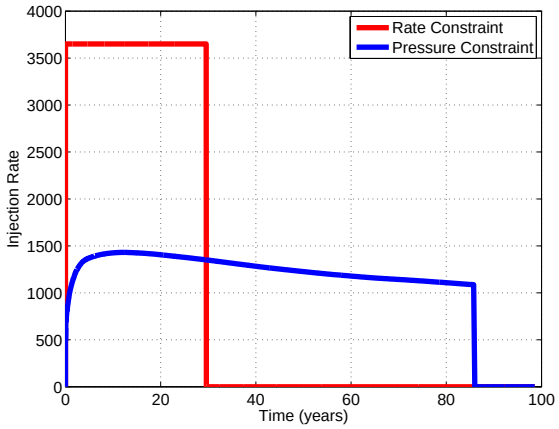

(c) Volumetric injection rate.

Figure 3: Aquifer and well pressure and injection rate in different injection scenarios shown for a test case.

to keep the 400 bar by reducing the injection rate. The well continues operation switching between these priorities until a total CO_2 volume of 40MM m^3 is injected into the medium. As soon as the total injected volume reaches this number, the injector will be shut from the bore-hole and no injection happens for the rest of simulation time.

4 Pressure analysis

We start by discussing the pressure responses we will use in our study for one particular realization. Then we do the full analysis by considering all of the 160 specified realizations, which are made by combining the geological variable levels discussed earlier[1]. Response plots are shown and discussed accordingly. Most of the reported results are chosen at 2.4 hours (0.1 day), i.e., at the beginning of injection. At that time, the system pressure response is higher compared to the later times when the pressure in the system drops to lower values (Figure 3b). Also, upto this time the same amount of CO_2 is injected in all cases, which allows for a fair comparison between cases.

Four types of responses are considered to be basis for the comparison between cases. One important question is how fast we can inject into a realization. To compare different cases, injection time is calculated considering a fixed total volume of injection in all models. Pressure behavior in the system is studied, by looking at aquifer average pressure and pressure drop across the well. An overpressure region is defined in

[1]Combining all the features and levels makes 162 cases. However, two cases were missing in the original data set.

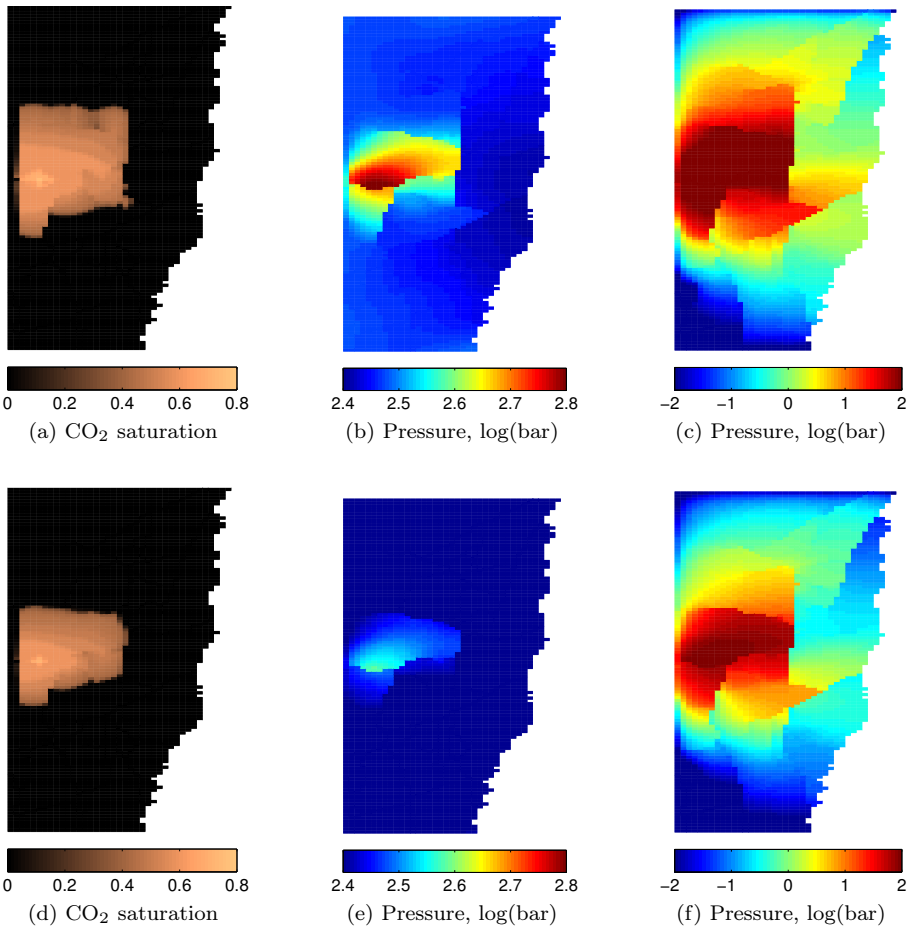

(a) CO_2 saturation (b) Pressure, log(bar) (c) Pressure, log(bar)

(d) CO_2 saturation (e) Pressure, log(bar) (f) Pressure, log(bar)

Figure 4: Responses at the middle of injection period (15 years). The first row corresponds to rate-constrained and the second row belongs to the pressure-constrained injection scenario. Figures c and f show the pressure build up from its initial value. Top view of last injection layer is shown in all figures.

which the volumetric spread of over-pressurized locations in the model is measured. Finally, the farthest place from the injection point that a pressure build up has reached is reported for each realization to see the impact of heterogeneity and channellings on how the pressure wave travels through the medium.

Figure 4 shows the pressure and saturation responses for the two injection scenarios in a selected case. This case has one lobe, parallel rock-type stratigraphy (i.e., low aggradation angle), and up-dip progradation. It is faulted with almost open faults and has high barrier level. Responses for the rate constrained scenario are given in Figures 4a, 4b and 4c, and those for the pressure constrained scenario are given in Figures 4d, 4e and 4f.

The pressure build-up in Figures 4c and 4f tells about heterogeneity impact on maintaining the pressure locally rather than transferring it across the medium. Comparing Figures 4b and 4c with Figures 4e and 4f, we see that imposing a pressure constraint on the injector significantly reduces the pressure build-up in the medium (as should be expected). However, the pressure disturbance propagates widely through the system in both cases (Figures 4c and 4f), far beyond the CO_2 invaded zones in Figures 4a and 4d.

4.1 Injection time

In the pressure-constrained scenario, the less the injectivity of the well is, the longer it will take to inject into the medium, keeping the pressure below the critical limit. In some of the cases it takes longer than 100 years (i.e., longer than the considered total simulation time) to inject the specified CO_2 volume. To compare

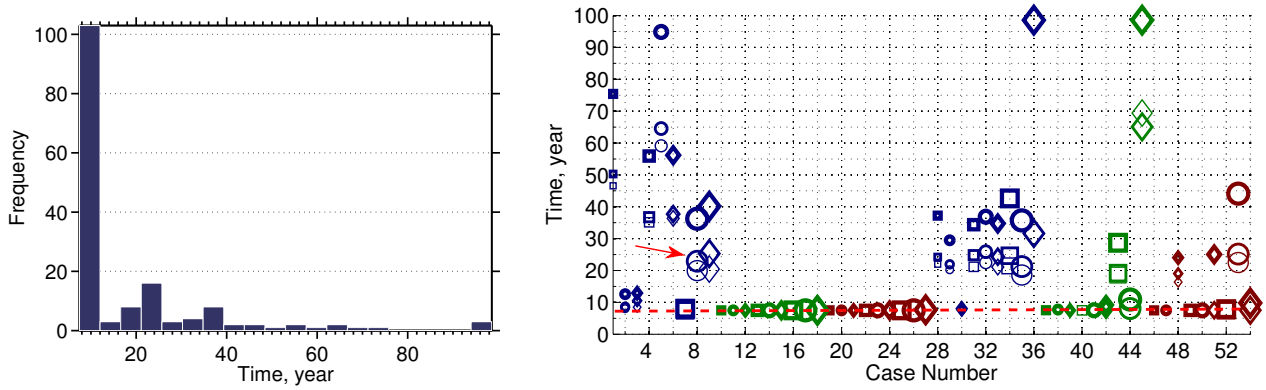

(a) Histogram of injection time in all cases.

(b) Case plot of injection time in all cases.

Figure 5: Time to inject quarter of the total specified CO_2 volume for all cases in the pressure-constrained scenario. The dashed red line in the right plot denotes the targeted injection time of 7.5 year, and the red arrow points to the case shown in Figure 4.

cases, we therefore calculate the time at which a quarter of the objective volume is injected. In all cases, this amount is injected within the total simulation time.

Figure 5 shows the injection time for all cases, using the pressure-constrained scenario. For many cases, the injector keeps the target rate, and thus, it completes the injection in 7.5 years (the dotted red line in the figure). The rest of the cases require longer injection time, due to the lower injectivity of the medium. This leads to pressure control in the injector, followed by a decrease in the injection rate.

Different codes used in the plot of Figrure 5 are describe in Table 1. Most of the cases with lower injection rates in the plot are colored blue, which translates to a low aggradation angle. Also cases with closed faults, denoted by thick markers, have (significantly) longerinjection time. Progradation effects are apparent on the higher aggradation cases: for some of the cases colored green and red in the second half of the plot in Figure 5, injection takes longer than the corresponding cases in the first half, which satusfy th etargeted injection. This means that down-dip progradation, independent of aggradation angle level, can result in lower injectivity.

4.2 Well and aquifer pressure

To see the overpressure caused by different heterogeneities, we compare cases for their average pressure and well pressure drop. Histograms of average aquifer pressure are shown in Figures 6a and 7a for different injection scenarios and average aquifer pressure at 2.4 hours after the start of injection is plotted for all cases in Figures 6b and 7b. In the rate-constrained scenario, high ranges of average pressure are observed (Figure 6b). Effects of aggradation angle, progradation and faulting are visible in the plot. Three clusters can be identified in the histogram of Figure 6a with medium, high and extreme pressure values. In Figure 7a, a small group of cases show lower pressures, while most of cases are distributed around the mean value (which reads 300 bar).

We define the average well pressure drop as the temporal average of the difference between the bottom-hole pressure and the average aquifer pressure.

Histograms of well pressure drop values are shown in Figures 8a and 9a. Higher values imply a poor injectivity of the medium. We see in Figure 8 that maintaining the target rate will in many cases require a huge pressure drop (up to 1400 bar in the worst cases) that would not be feasible nor possible to obtain. Pressure control on the injector reduces the range of pressure drop variation below 170 bar. The average injector pressure drop is plotted for all cases in Figures 8b and 9b.

Two regions can be identified in the medium, the region near the injection point; and the part of aquifer which is far from the injection point. The well-bore pressure is effected directly by heterogeneities in the near

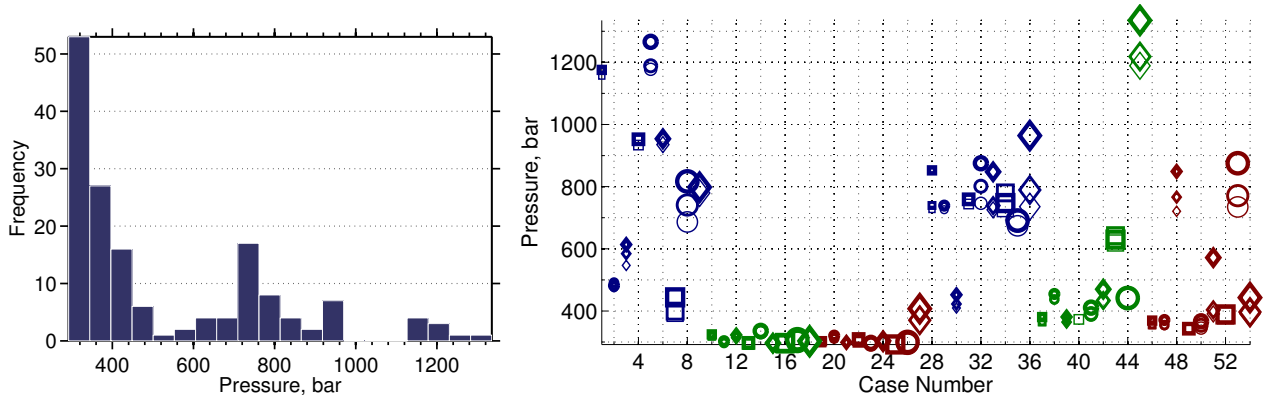

(a) Histogram of pressure values.

(b) Case plot of pressure values.

Figure 6: Average aquifer pressure for all cases in the rate-constrained scenario.

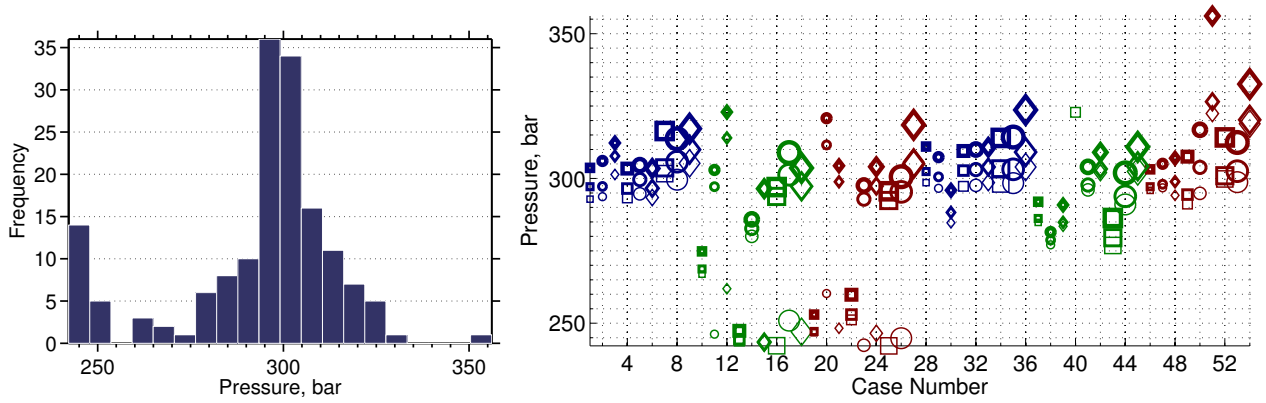

(a) Histogram of aquifer pressure values.

(b) Case plot of aquifer pressure values.

Figure 7: Aquifer average pressure for all cases in the pressure-constrained scenario.

well-bore region, while the larger scale region influences the average aquifer pressure. Pressure drop variations in Figures 8a and 8b are influenced by the heterogeneity near the well-bore, where the reaction to injecting a fixed amount of CO_2 starts by a local pressure build-up. Heterogeneity on the scale of aquifer plays a considerable role in the range of variations in Figures 9a and 9b. In the pressure-constrained scenario, local pressure is controlled by putting a constraint on the well. Hence, the pressure drop variations are controled bay the average aquifer pressure.

As we see in Figure 8b, low aggradation angle and down-dip progradations result in a poor injectivity and high pressure buildup in the injector. Vertical transmissibility drops dramatically for low aggradation angles [1]. This restricts the pressure transfer within the injection layer, and therefore the pressure builds up locally around the well. Moreover, in cases with down-dip progradation the low permeabilty rocks surrounding river branches near the injector result in a local pressure buildup.

A group of cases in Figure 9 have a relatively low pressure drop of less than 50 bar. These cases have a good injection quality, and the pressure is released through open boundaries easier than other cases. The rest of the cases show higher pressure drop because of the heterogeneities in the larger scale, far from the injector. These results are obtained for a fixed injection location to examine the heterogeneity impact on injectivity. Herein, we aim to honor the geological uncertainty. In practice, the injector must be drilled and completed in the best formation with highest possible injectivity.

Faults influence both local pressure build-up near the injector as well as the average aquifer pressure. Therefore, they have a visible trend in many cases in Figures 8b and 9b (for example, see the three cases

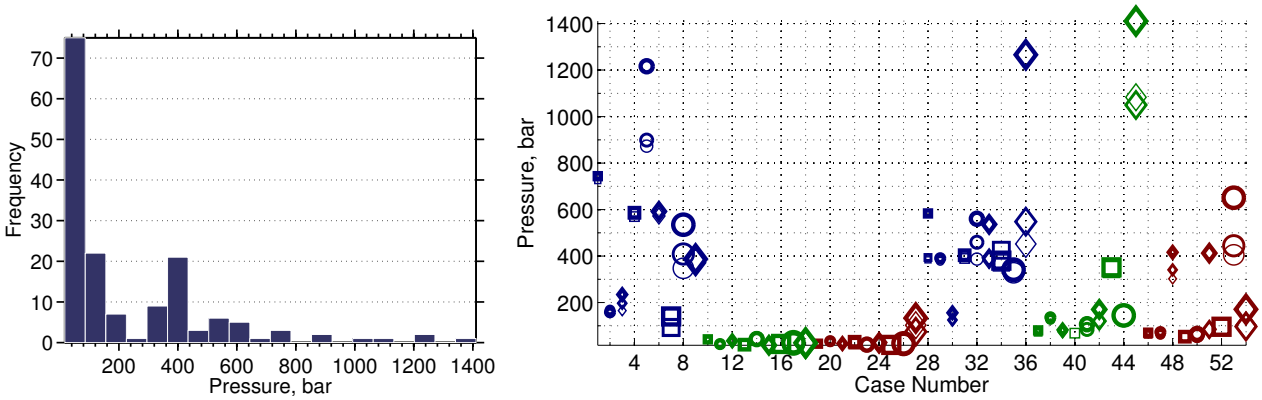

(a) Histogram of pressure drop values.

(b) Case plot of pressure drop values.

Figure 8: Average of injector pressure drop for all cases in the rate-constrained scenario.

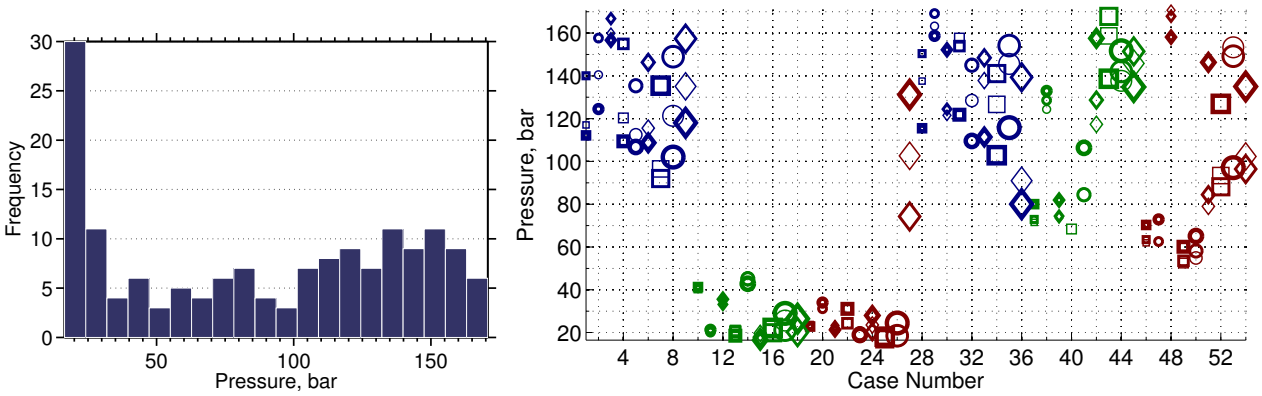

(a) Histogram of pressure drop values.

(b) Case plot of pressure drop values.

Figure 9: Average of injector pressure drop for all cases in the pressure-constrained scenario.

denoted by red circles in the right end of Figure 8b). This is specially more apparent in cases with high level of barriers.

4.3 Pressurized region

Here, we study the overpressure distribution in the medium. An absolute pressure limit of 300 bar is set as threshold, such that all cells with a pressure higher than this value form a region that is called the pressurized region. The volumetric fraction of this region is defined by the ratio of pressurized volume to the total volume of all active cells in the model.

Histogram and case plot of the pressurized volume fraction at the start of injection are given in Figure 10. Here, we clearly see that low agrradation angle is very influential in the pressure buildup in the injection zone. A group of cases with low aggradation angle have a relatively large pressurized region in Figure 10b. However, also there are number of cases in Figure 10b that have a relatively low pressurized fraction. In these cases, the medium is conductive toward the open boundaries and the heterogeneity in the medium does not cause a major pressure buildup. Other observation in Figure 10b is the progradation effect; down-dip progradation, shows a rise in pressurized fraction for higher aggradation angles.

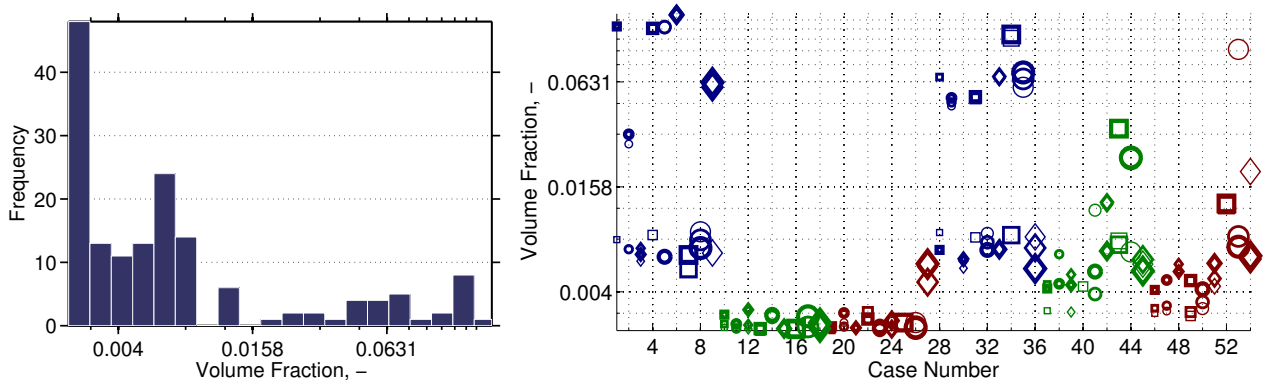

(a) Histogram of pressurized volume fractions.

(b) Case plot of pressurized volume fractions.

Figure 10: Pressurized volume fraction for all cases in the rate-constrained scenario.

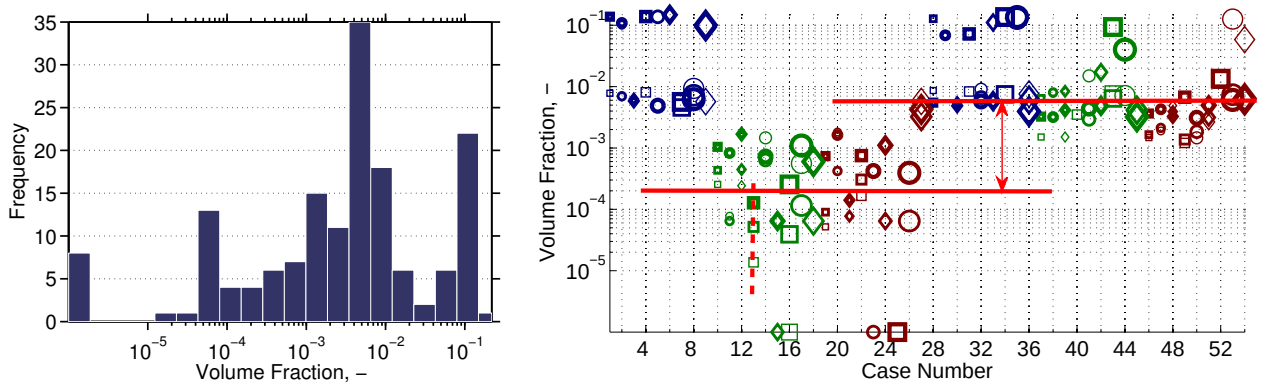

(a) Histogram of build-up volume fractions.

(b) Case plot of build-up volume fractions.

Figure 11: Build-up volume fraction for all cases in the rate-constrained scenario.

4.4 Build-up region

To study the pressure change, and how a pressure disturbance spreads through the medium, we use another metric. We calculate the pressure change by subtracting the initial pressure at each location from the current pressure. Different realizations are compared for the size of a region, which we call the buildup region, where the pressure increases from its initial value by 10 bar. The value 10 bar is chosen to make sure that the region has not reached the boundaries in any of the studied cases. The smaller the buildup region is, the less volume will be exposed to pressure change in the aquifer (Figure 11).

Higher pressure in the medium will obviously cause a larger buildup region. Impact of progradation on the pressure build-up is illustrated in Figure 11b. Up-dip progradation shows a relatively lower pressure buildup compared to down-dip progradation cases. We also see that aggradation dominates this effect, where cases with low aggradation angle show the same build-up pressure for both types of progradation directions (Note the blue colored markers that dont follow the lines in Figure 11b).

Several cases in Figure 11b show a trend for the fault parameter. The dashed line in the figure shows the trend of build-up pressure increase due to fault feature variations in three cases. Faulting changes the geometry of layers and puts different layers adjacent to each other. This enhances the connectivity in the medium. Local heterogeneities and closed faults around the injector make a larger build-up region, because

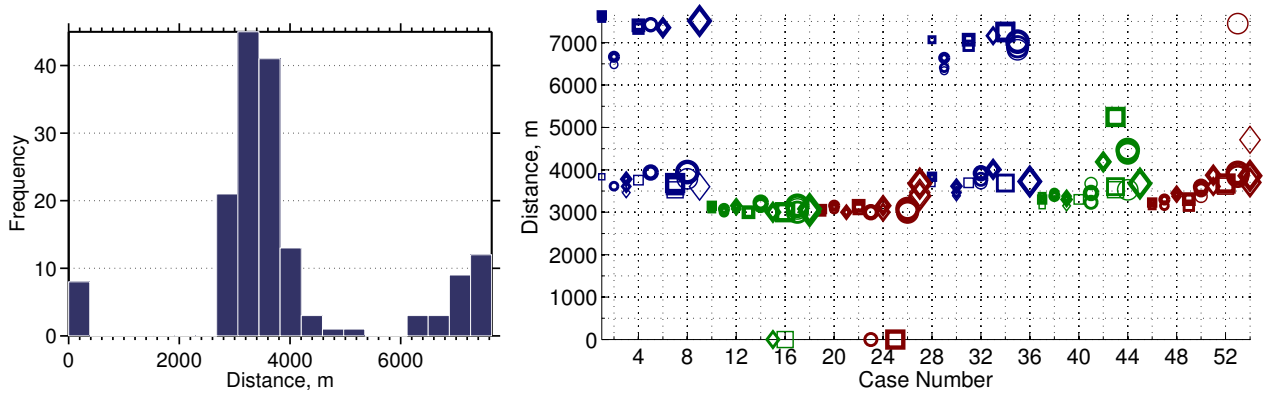

(a) Rate-constrained scenario.

(b) Rate-constrained scenario.

Figure 12: The farthest pulse of the pressure build-up distance from the injection point for all cases in the rate-constrained scenario.

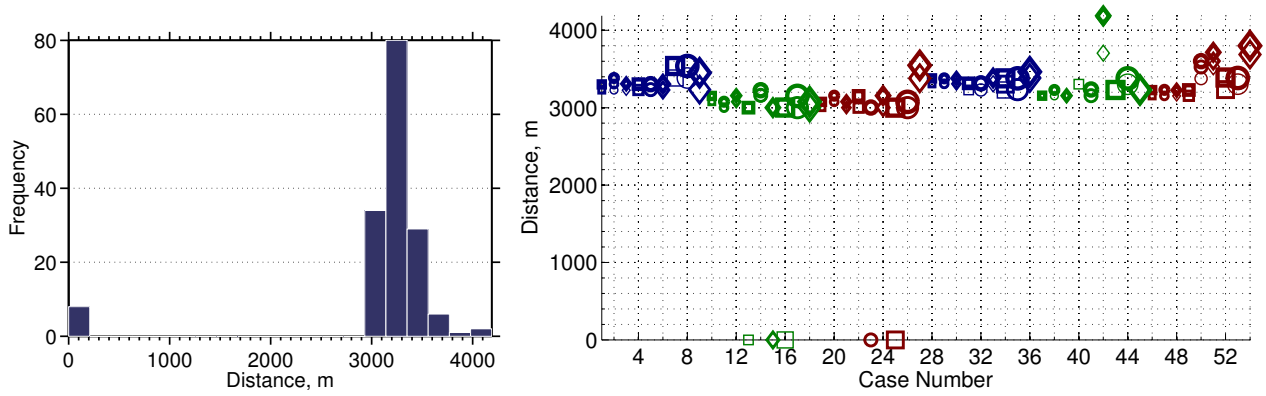

(a) Pressure-constrained scenario.

(b) Pressure-constrained scenario.

Figure 13: The farthest pulse of the pressure build-up distance from the injection point for all cases in the pressure-constrained scenario.

they cause higher pressure build-up in the domain. In these cases, the effect of heterogeneity of different scales, namely on the scale of near injector and far from injector, are combined causing a larger buildup fraction.

4.5 Farthest pulse

As discussed earlier, irregular geometries like faults and unconformities can lead to pressure spread in the domain. Looking at the volume fraction of pressurized and buildup regions helps in comparing cases for their pressure conductivity, but it does not show the extent of pressure spread in the medium. For that reason, we also look at the farthest cell from the injection point that falls within the buildup region defined earlier.

Figures 12 and 13 show the farthest pressure build-up distances from the injector in different injection scenarios. In Figure 12a, three groups of cases can be identified: cases with zero distance of farthest pressure build-up pulse, cases with medium distances, and those with large distances from the injection point. Three specific cases are chosen as samples from each of the groups. In the first group, the pressure does not exceed the 10 bar threshold from its initial value in the medium. For these cases, the injector is placed in a permeable region and the medium is conductive towards open boundaries (Figure 14a). Hence, the imposed injection pressure does not build up, neither locally around the well nor globally in the aquifer scale. The second group

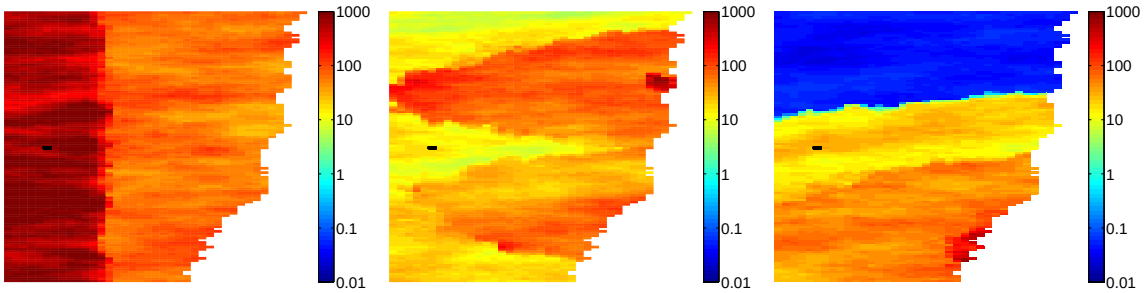

Figure 14: Permeability of three cases in unit millidarcies shown in color, and the Well location is illustrated with black color on each plot . Top view is shown in the plots.

in Figure 12a have a medium range of $3-4$ km of distances from the injection point. Heterogeneity in these cases is not making a high pressure build-up around the injector and throughout the medium (Figure 14b).

In the third group, low permeability rocks in the injection layer cause a high pressure build-up around the injection point. If the injector zone is isolated by sealing heterogeneities, the pressure rises in a limited region. However, if the well is connected throughout the medium, and the heterogeneities in the aquifer scale contain relativly low permeability rocks, the pressure build up spreads wider in the aquifer. In Figure 14c, the injection point is located close to a low transmissibility rock. This rises the pressure level in the injector. Other parts of the aquifer are connected with poor quality rocks, resulting in a wide build-up region.

The farthest pulse distance ranges from 8 km to about 10 km in the extreme cases. By controlling the injection pressure, the maximum shrinks to less than 5 km (Figure 13a).

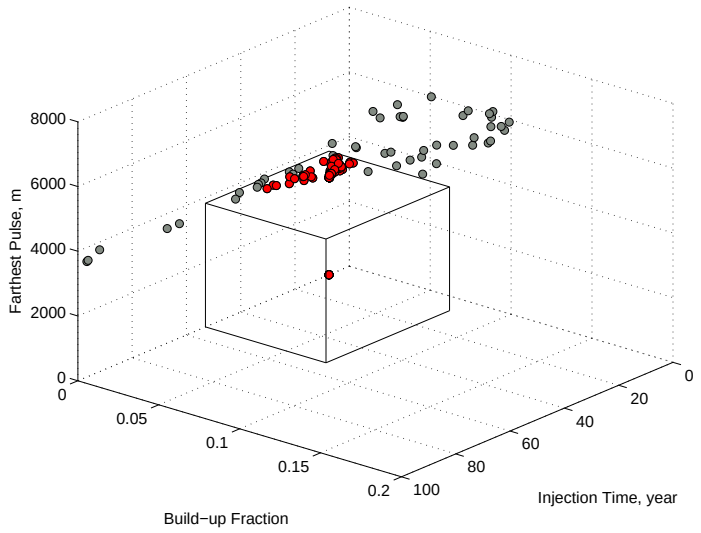

Figure 15: Pressure criteria implemented to filter the acceptable cases. Cases below the critical limits are plotted in red and cases exceeding the limits are plotted in gray.

5 Discussion

So far, we reported the model responses that measure the pressure rise and pressure disturbance propagation in the domain. Pressurized volume fraction indicates the actual high pressures that may occur in an injection operation. Build-up volume fraction and farthest pulse are indicators of how the pressure disturbance is

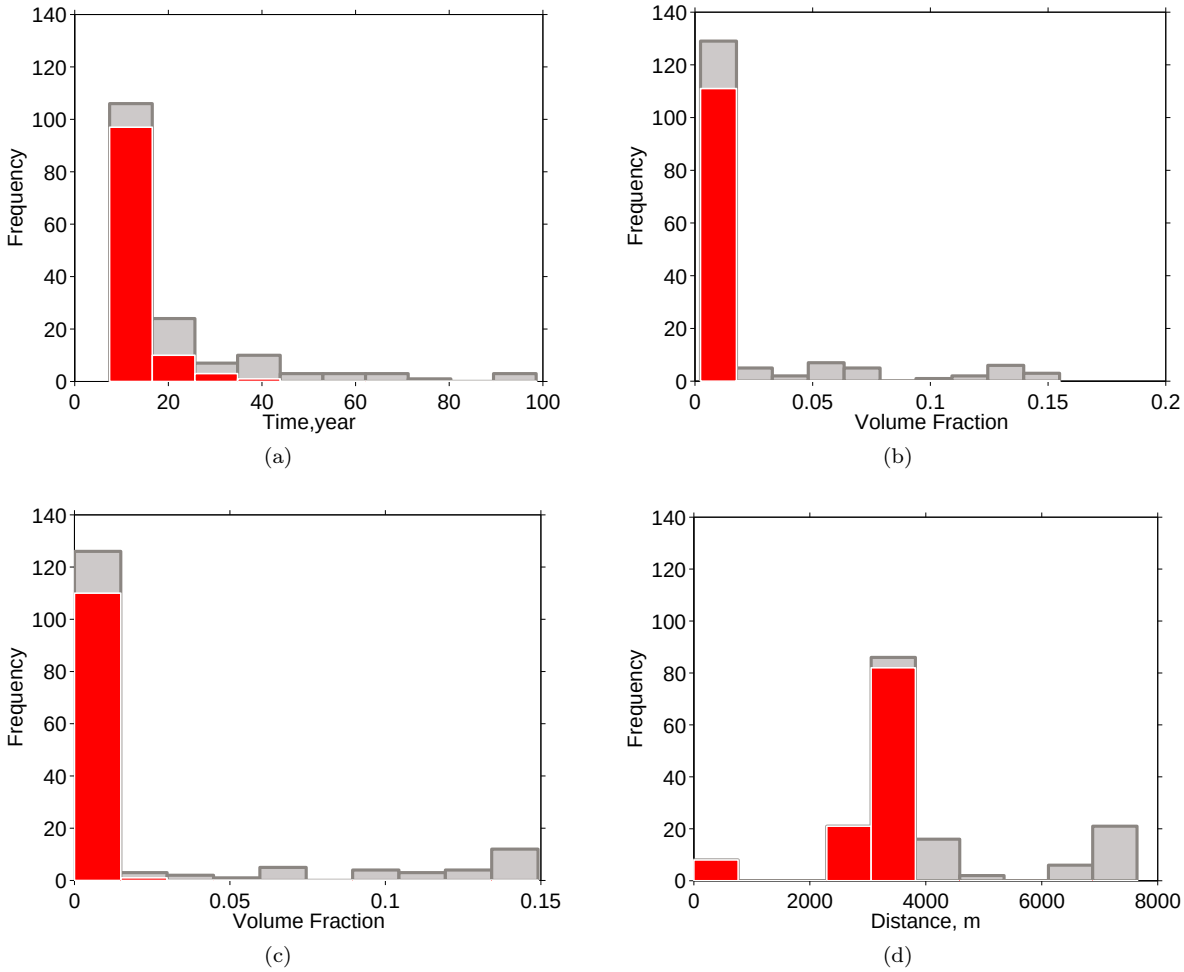

Figure 16: The histogram of filtered cases (coloered in red) compared with the histogram of all cases for different pressure responses: a) Injection time, b) Pressurised volume fraction, c) Build-up volume fraction, and d) Farthest pulse distance from the injection point.

spread in the system. We are interested in limiting both the pressure increase and the area of well pressure influence in the aquifer.

In most of the results, aggradation angle, progradation direction and faults play a major role in the pressure behavior. For low aggradation angle, geological layers are made of rock types piled in a parallel stratigraphy. Thus, efficient vertical permeability is the harmonic average of these layers. If any of these layers contains a low permeability rock, this will result in a low vertical permeability. Injecting into a limited space sealed vertically, increases the pressure in the injection point.

Progradation direction can dominate the pressure behavior. It is very important to locate the injector in a high permeability zone is connected to other parts of the domain via permeable channels. Injecting into the river side of a shallow-marine depositional system, may end up into locating the injection point in a low quality rock between river branches joining the sea. This rises the pressure significantly near the injection point and can result in a high well-bore and aquifer pressure.

Structural deformations due to faulting process can increase the connectivity in the medium. If the transmissibity in the aquifer scale is high, the injection pressure releases through the open boundaries. However, if the injection area is surrounded by low quality medium, the pressure rises in the aquifer and the connectivity enhanced by fault geometries spread the build-up region in the domain. On the other hand, sealing faults result in high pressure within closed zones around the injection point. However, they may limit the pressure disturbance propagation in the domain.

From an operational perspective, pressure limits must be set to keep the operations within safe margins. One approach to study the safety of an operation could be setting critical limits on the pressure responses measured here. This limit is used to filter cases with desirable/acceptable pressure behavior. The critical margins are inferred from the realistic operational requirments. In our pracice, we assume these margins to be 53 years for the injection time, 0.0787 for the pressurised volume fraction, 0.0745 for the build-up volume fraction, and 3822 m for the farthest pulse distance from the injection point. These values are picked from the middle points of range of variations in the results. By these assumptions, 49 cases out of total number of 160 cases exceed the critical limits.

Figure 15 shows the cases filtered by the pressure criteria. In Figure 15, the pressurized volume fraction is also considered in the filtration, though it is not shown in the plot axes. The plot shows that most of the cases that pass the filtering are concentrated in a region of low build-up fraction values. Figure 16 reports the histogram of filterd cases in comparison with the histogram of all studied cases for each response.

6 Conclusion

This work is a part of comprehensive sensitivity studies to assess the impact of geological heterogeneity on CO_2 injection and early migration. The aim of this study is to define preventing measures that can be used to avoid high pressures and the damages accompanied by them during the injection operations. Simulation responses related to the pressure behavior in the system are defined and calculated for two CO_2 injection scenarios. Geological variations in shallow-marine depositional systems are examined by using large number of realizations representing a spectrum of sedimentological and structural parameters. Operational critical values are considered for the defined preventive measures.

Most of the studied responses, show relatively a higher sensitivity to aggradation, progradation and faulting. Low aggradation angle keeps the flow restricted in a limited space. In cases with low rock quality in injection layers, pressure builds up in the well-bore. Injecting in down dip progradation, normally ends up in a higher pressure buildup and lower injectivity. In the down dip progradation, the majority of the region around injection point is made of low quality rock. Faults change the geometrical structure of the medium and they put different layers in contact. Pressure disturbance can leak through faults to larger distances from injection point. Closed faults can significantly reduce the injectivity quality.

The work-flow of pressure study demonstrated here can be used in a specific studies in the context of geological uncertainty. The work-flow can be used for other depositional systems and diffrent values for operational limits can be used, which might lead to outcomes different than the results reported here.

References

[1] M. Ashraf, K.A. Lie, Nilsen, and A. Skorstad. Impact of geological heterogeneity on early-stage CO_2 plume migration: Sensitivity analysis. In *ready for submission*, 2012.

[2] M. Ashraf, K.A. Lie, H.M. Nilsen, J.M. Nordbotten, and A. Skorstad. Impact of geological heterogeneity on early-stage CO_2 plume migration. In *CMWR*, 2010.

[3] B. Cailly, P. Le Thiez, P. Egermann, A. Audibert, S. Vidal-Gilbert, and X. Longaygue. Geological storage of CO_2: A state-of-the-art of injection processes and technologies. *Oil & Gas Science and Technology*, 60(3):517–525, 2005.

[4] A. Cavanagh and N. Wildgust. Pressurization and brine displacement issues for deep saline formation CO_2 storage. *Energy Procedia*, 4:4814–4821, 2011.

[5] J.A. Howell, A. Skorstad, A. MacDonald, A. Fordham, S. Flint, B. Fjellvoll, and T. Manzocchi. Sedimentological parameterization of shallow-marine reservoirs. *Petroleum Geoscience*, 14(1):17–34, 2008.

[6] T. Le Guenan and J. Rohmer. Corrective measures based on pressure control strategies for CO_2 geological storage in deep aquifers. *International Journal of Greenhouse Gas Control*, 2010.

[7] T. Manzocchi, J.N. Carter, A. Skorstad, B. Fjellvoll, K.D. Stephen, JA Howell, J.D. Matthews, J.J. Walsh, M. Nepveu, C. Bos, et al. Sensitivity of the impact of geological uncertainty on production from faulted and unfaulted shallow-marine oil reservoirs: objectives and methods. *Petroleum Geoscience*, 14(1):3–11, 2008.

[8] J.D. Matthews, J.N. Carter, K.D. Stephen, R.W. Zimmerman, A. Skorstad, T. Manzocchi, and J.A. Howell. Assessing the effect of geological uncertainty on recovery estimates in shallow-marine reservoirs: the application of reservoir engineering to the SAIGUP project. *Petroleum Geoscience*, 14(1):35–44, 2008.

[9] J.P. Nicot. Evaluation of large-scale CO_2 storage on fresh-water sections of aquifers: an example from the Texas Gulf Coast Basin. *International Journal of Greenhouse Gas Control*, 2(4):582–593, 2008.

[10] C. Oldenburg. Comments on Economides and Ehlig-Economides,"Sequestering carbon dioxide in a closed underground volume" SPE 124430, October 2009. 2010.

[11] J. Rutqvist, J. Birkholzer, F. Cappa, and C.-F. Tsang. Estimating maximum sustainable injection pressure during geological sequestration of CO_2 using coupled fluid flow and geomechanical fault-slip analysis. *Energy Conversion and Management*, 48(6):1798–1807, 2007.

[12] J. Rutqvist and C.F. Tsang. A study of caprock hydromechanical changes associated with CO_2 injection into a brine formation. *Environmental Geology*, 42:296–305, 2002. 10.1007/s00254-001-0499-2.

[13] L.G.H. van der Meer. Investigations regarding the storage of carbon dioxide in aquifers in the Netherlands. *Energy Conversion and Management*, 33(5-8):611–618, 1992.

[14] L.G.H. van der Meer. The conditions limiting CO_2 storage in aquifers. *Energy Conversion and Management*, 34(9-11):959–966, 1993.